SSC23-III-05

# Prototype testing results of charged particle detectors and critical subsystems for the ESRA mission to GTO

Carlos A. Maldonado, Jonathan Deming, Brooke N. Mosley, Justin McGlown, Anthony Nelson, Philip A. Fernandes, Anthony J. Rogers, Douglas Patrick, Martin Kroupa, Michael Caffrey, Susan Mendel, Kerry Boyd, August Gula, Kim Katko, Markus P. Hehlen, Daniel Arnold, Jonathan Barney, Ted Schultz, Daniel B. Reisenfeld, Ruth Skoug, Angus Guider, Michael Holloway, Heidi Morning, John T. Steinberg, Erik Krause, Andrew Kirby, Darrel Beckman, Justin Tripp, Keith S. Morgan, Zachary Miller, Robert Merl, Paul S. Graham, Joshua Ortner, Quinten Cole, Chuck Clanton, Brian A. Larsen, Tom Fairbanks, Jeffrey George, Rory Scobie, Kasidit Subsomboon, Kristina McKeown, Katherine Alano, John Michel, Darren Harvey, Andrew Harvilla, and Donathan Ortega

Los Alamos National Laboratory
Los Alamos, NM; 505-667-1933
cmaldonado@lanl.gov

## ABSTRACT

The Experiment for Space Radiation Analysis (ESRA) is the latest of a series of Demonstration and Validation (DemVal) missions built by the Los Alamos National Laboratory, with the focus on testing a new generation of plasma and energetic particle sensors along with critical subsystems. The primary motivation for the ESRA payloads is to minimize size, weight, power, and cost while still providing necessary mission data. These new instruments will be demonstrated by ESRA through ground-based testing and on-orbit operations to increase their technology readiness level such that they can support the evolution of technology and mission objectives. This project will leverage a commercial off-the-shelf CubeSat avionics bus and commercial satellite ground networks to reduce the cost and timeline associated with traditional DemVal missions. The system will launch as a ride share with the DoD Space Test Program to be inserted in Geosynchronous Transfer Orbit (GTO) and allow observations of the Earth's radiation belts. The ESRA CubeSat consists of two science payloads and several subsystems: the Wide field-of-view Plasma Spectrometer, the Energetic Charged Particle telescope, high voltage power supply, payload processor, flight software architecture, and distributed processor module. The ESRA CubeSat will provide measurements of the plasma and energetic charged particle populations in the GTO environment for ions ranging from ~100 eV to ~1000 MeV and electrons with energy ranging from 100 keV to 20 MeV. ESRA will utilize a commercial 12U bus and demonstrate a low-cost, rapidly deployable spaceflight platform with sufficient SWAP to enable efficient measurements of the charged particle populations in the dynamic radiation belts.

## BACKGROUND & INTRODUCTION

The Experiment for Space Radiation Analysis (ESRA) is the latest of a series of Demonstration and Validation (DemVal) missions built by the Los Alamos National Laboratory (LANL), with the focus on testing a new generation of plasma and energetic particle sensors [1, 2, 3, 4]. Space plasma and energetic charged particle instrument design has traditionally been guided by the philosophy of "build to performance," where science objectives and measurement requirements are developed prior to the science instruments [5]. In this design paradigm the required resources for the instrument are secondary considerations. Over the years this methodology has resulted in expensive instruments with high resource requirements making it difficult for smaller missions, operating under ever increasing fiscal constraints, to manifest these exquisite sensors. The primary motivation for the ESRA payloads is to minimize size, weight, power, and cost (SWaP-C) while still providing necessary mission data. These new instruments will be demonstrated by ESRA through testing and on-orbit operations to increase their technology readiness level (TRL) such that they can support the evolution of technology and mission objectives.

This project will leverage a 12U commercial off-the-shelf (COTS) CubeSat avionics bus from NanoAvionics and commercial satellite ground networks from KSAT to reduce the cost and timeline associated with traditional DemVal missions. The commercial sector continues to rapidly increase the capability of SmallSat platforms while simultaneously reducing risk and cost. Subsequently, the space community has witnessed a tremendous growth in satellite constellations for scientific [6, 7, 8], commercial [9, 10], and government

applications [11]. The ESRA mission has been presented at the Space Experiments Review Board (SERB), including the SEED [12] and will launch as a ride share with the DoD Space Test Program (STP) to be inserted in Geosynchronous Transfer Orbit (GTO). This mission orbit will allow for observations of the space plasma and charged particle populations from low-Earth orbit (LEO) to geosynchronous Earth orbit (GEO), including the Earth's radiation belts. Operation in this environment will provide flight heritage of critical technologies in the most stressing conditions for near-Earth orbits.

The ESRA CubeSat consists of two science payloads and several critical subsystems: the Energetic Charged Particle (ECP) telescope, the Wide field-of-view Plasma Spectrometer (WPS), high voltage power supply (HVPS), payload processor (PP), flight software architecture, and distributed processor module (DPM). The LANL-designed payload processor will control the experiment, record the data, and communicate with the CubeSat avionics while the DPM will provide limited processing at the sensor head locations and packetize data. The DPM provides the capability to mount multiple sensors in nontraditional configurations, i.e. sensor heads not co-located, in order to maximize the ability to conform the sensor suite to any host and optimize fields-of-view. The ESRA CubeSat will provide measurements of the plasma and energetic charged particle populations in the GTO environment for ions ranging from ~100 eV to ~1000 MeV and electrons with energy ranging from 100 keV to 20 MeV. The ESRA mission will serve to demonstrate the potential of CubeSats for both science and space weather monitoring in the radiation belts.

## SCIENCE PAYLOADS

### *Energetic Charged Particle (ECP) Detector*

The Energetic Charged Particle (ECP) telescope measures protons and electrons over a broad range of energies (100 keV – 1000 MeV for protons, and 100 keV – 20 MeV for electrons) [13, 14, 15]. The telescope design incorporates five detectors in a stack up: two thin Si detectors (80 µm thick), two thick Si detectors (1500 µm thick), and one GAGG(Ce) ($Ce^{3+}$-doped $Gd_3Al_2Ga_3O_{12}$) scintillator (1 cm thick) with a Hamamatsu S3590-08 PhotoDiode (PD). The computer aided design (CAD) model of the ECP telescope is shown in Figure 1, illustrating the detector stack-up order. The sensitive detectors in the telescope are shielded with tungsten, shown in grey, and aluminum, shown in yellow. To lower the background signal and improve signal to noise ratio of the telescope, an aluminum collimator with tungsten discs is positioned in front of the telescope.

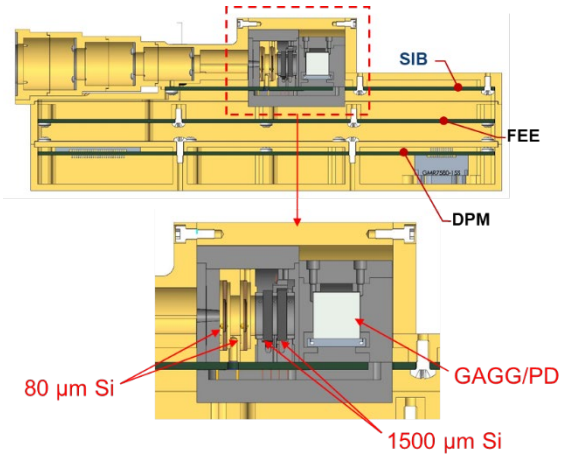


**Figure 1. CAD model cutaway of the ESRA ECP telescope.**

Each channel has dedicated read-out electronics, which are integrated into the body of the telescope. Three electronic boards comprise each electronics module and are optimized to fit the allocated footprint and minimize noise and heat cross-talks. The board closest to the detectors is the Sensor Interface Board (SIB) which provides a low-noise interface between the electronics and detectors. The SIB also provides detector biasing and monitors the leakage current. The Front-End Electronics (FEE) board incorporates junction-gate field-effect transistors (JFETs) and charge sensitive preamplifiers to amplify detector signals. After the amplified signals are shaped and filtered, each signal is then sampled by an analog-to-digital converter (ADC) with a sampling rate of 80 MHz. This digital signal is passed to the Distributed Processing Module (DPM), where a field-programmable gate array (FPGA) analyzes the signal. Compared to the standard application with the "peak hold" approach, this fully digital approach enables much more sophisticated signal processing, resulting in higher acceptable count rate due to "in-flight" baseline restoration.

A prototype of the telescope has been assembled, with individual detectors calibrated using radioactive sources. The prototype was tested at the Brookhaven National Laboratory (BNL) Single Event Upset (SEU) test facility with proton beams from the Tandem Van de Graaff accelerator, demonstrating both the operation of all detectors in coincidence, and total energy reconstruction of the proton beam. Figure 2. Collected waveforms of prototype telescope with proton beam shows the detector signals from a 28 MeV proton beam, and Figure 3. Summed energy from 10 MeV proton shows the summed energy from the first 3 detectors for a 10 MeV beam. The discrepancy in energy is due to energy loss from the light tight window, silicon dead layers, and conformal coating around the detectors.

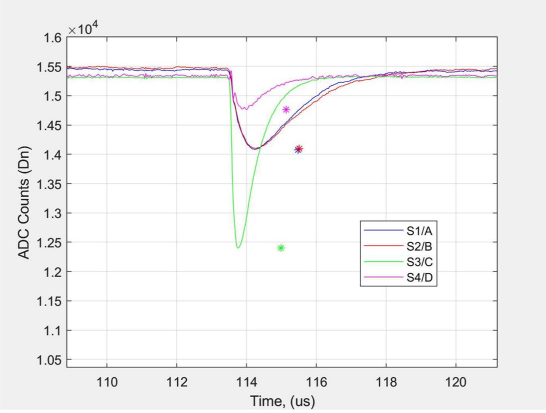


**Figure 2. Collected waveforms of prototype telescope with proton beam**

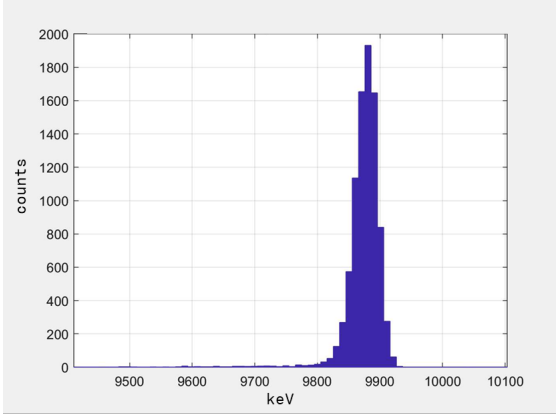


**Figure 3. Summed energy from 10 MeV protons depositing energy in 3 detector layers.**

### *Wide field-of-view Plasma Spectrometer (WPS)*

The Wide field-of-view Plasma Spectrometer (WPS) measures incident ion and electron energies and incident angles over a nearly 2π field-of-view (FOV), and is described in detail by Skoug, et al. [16]. This design acquires a complete plasma measurement in a single voltage sweep and is designed to measure a broad FOV without relying on spacecraft spin or deflection plates, both of which require additional time and/or resources to obtain full distribution measurements. The WPS sensor presents one of the most revolutionary steps forward in plasma spectrometer design since the development of the "top-hat" electrostatic analyzer by Carlson, et al. in 1984 [17]. The WPS is a candidate for the next generation of space environment detectors for Los Alamos missions.

The WPS instrument concept was first introduced in detail by Skoug, et al. [16] and in this section we briefly paraphrase their description. The design is based on a pinhole camera concept and the sensor head consists of the entrance aperture dome, the energy-angle (EA) charged particle filter plate, and the bullet structure at the center of the EA filter plate, shown in Figure 2. The 2-D imaging anode subsystem includes a transmissive grid of electroformed nickel mesh, microchannel plate (MCP) detector, a position sensitive crossed delay line (XDL) anode and associated front-end electronics (FEE). The combination of the MCP/XDL anode and FEE will serve as a 2-D imaging anode which will be used to detect the incident ions [18, 19, 20, 21, 22].

Ions enter the pinhole aperture with incident energy $E$, polar angle $\alpha$, and azimuthal angle $\phi$. After passing through the pinhole aperture the ion trajectories are deflected by the electric field created by biasing the EA filter plate to electrostatic potential $V_{fp}$, while the upper dome is held at spacecraft ground. The ions reach the EA filter plate at radial distance $r$ and angle $\beta$. The EA filter plate is populated with a series of channels whose bias angle $b$ varies as a function of radius $r$. Only ions that reach the filter plate with the appropriate angle, i.e. $\beta = b$, can successfully traverse the channel in the filter plate. Upon exiting the filter plate, the ions pass through the negatively biased transmissive grid which primarily serves to enhance detection efficiency by suppressing secondary electrons emitted from the MCP surface. Each incident ion creates an electron avalanche within the MCP. This electron cloud exits the bottom of the MCP and impacts the XDL, generating a measurable current pulse. This signal is transmitted to the FEE, which uses precision timing measurements to reconstruct the 2-D spatial location of the incident particle. The radial location maps to the incident polar angle of the ion $\alpha$; the azimuthal location maps to the incident azimuthal angle of the ion $\phi$; and the EA filter plate voltage $V_{fp}$ maps to the incident energy of the ion $E$. The EA filter plate voltage $V_{fp}$ is then swept over a range of voltages to obtain the full energy distribution of incident ions. In this way, ($V_{fp}$, $r$, $\beta$) from WPS maps to ($E$, $\alpha$, $\phi$) of the incident ion distribution [2].

For use on a resource constrained CubeSat platform such as ESRA, we have reduced the WPS design as described by Skoug, et al. [16] to the WPS Wedge. Specifically, the fully realized WPS measures a nearly 2π steradian FOV with an azimuth range of 360° while the WPS Wedge measures nearly π/2 steradian FOV with an azimuth range of 89°. The WPS Wedge will measure ions with incident energies spanning 0.10–35 keV with targeted energy resolution $\Delta E/E \leq 0.15$. The full FOV is 89° × 60° with an angular resolution ≤ 10°.

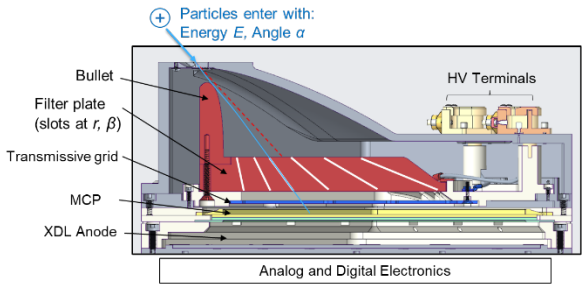


**Figure 2. Cross-sectional schematic of WPS CAD illustrating operation [2].**

A prototype assembly of the WPS instrument was tested using a monoenergetic proton beam to characterize energy and angular response. The internals of the WPS prototype, including filter plate and bullet (red dot and arc, respectively), are shown in Figure 4 (top). The WPS prototype was installed into a vacuum chamber on controllable motion stages, allowing precise (<0.25° resolution) orientation of the WPS aperture relative to the incident proton beam. Figure 4 (middle) shows the MCP/XDL readout of data acquired during the calibration campaign. The brownarc identifies the edge of the filter plate. Measured protons from the incident beam are shown (blue circle labeled "Signal"), as are some persistent noise signatures from the MCP (orange).— These noise signatures are fortuitously located predominantly outside of the portion of the MCP utilized for this experiment. By using the motion stages to rotate the instrument aperture relative to the incident ion beam, we demonstrated response along a full channel of the WPS filter plate (purple dots), as well as radial response (red dots).

We then characterized the instrument response to proton beams of different energies: 1, 8, 18, and 30 keV, spanning much of the intended instrument energy range. Six incident beam angles were used to collect data at each energy, allowing for characterization of the coupling of energy response and angular response in WPS. This is shown in Figure 3 (bottom); note the orientation of WPS has changed in these figures and the bullet is now in the top-left corner (green dot). Efforts to incorporate the characterization results into electro-optical models and determine overall geometric factors are currently underway.

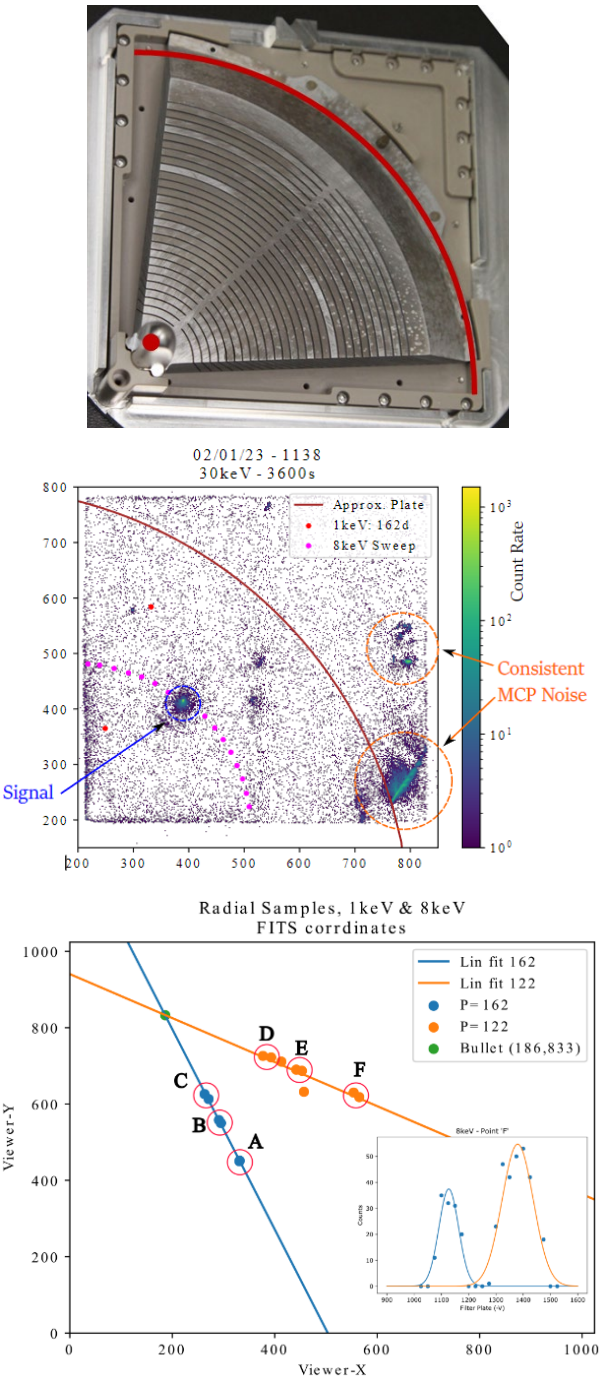


**Figure 3. (top) Top view of the EA filter plate with bullet location and outer edge indicated in red, (middle) prototype 2-D imaging anode data, and (bottom) prototype data as a function of beam energy and angle.**

## CRITICAL SUBSYSTEMS

As a DemVal mission, ESRA will rapidly increase the TRL of next generation critical subsystems. These

include a CubeSat compatible high voltage power supply, distributed processing architecture, payload processor, and flight software architecture which are described in more detail in the literature [2, 1]. The LANL-designed payload processor will control the experiment, record the data, and communicate with the CubeSat avionics while a DPM will provide limited processing at the sensor head locations and packetize data. The HVPS system will provide static and dynamic high voltage to the sensor payloads and the Flight Software (FSW) will control command & data handling. The top-level block diagram of the ESRA system is shown in Figure 4.

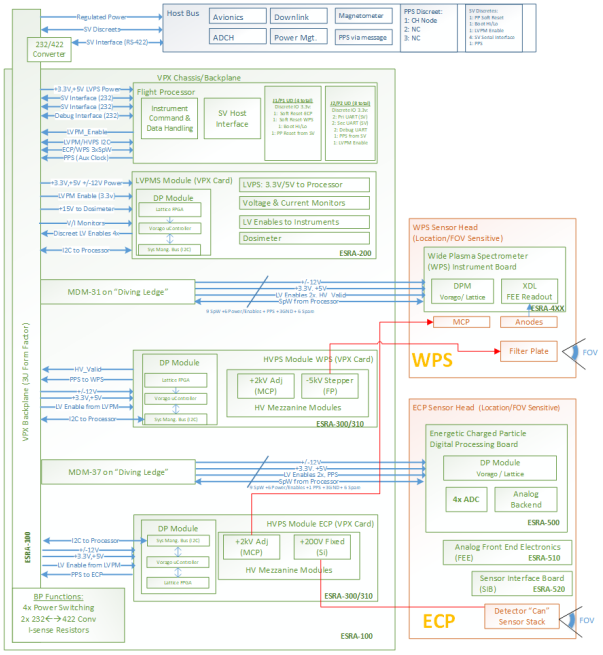


**Figure 4. ESRA Top Level System Block Diagram.**

### *Compact Modular High Voltage Power Supply (HVPS)*

The ESRA Space High Voltage Power Supply team is currently developing a compact modular HVPS that adheres to the 3U SpaceVPX (ANSI/VITA 78) specification using a conduction-cooled frame compliant with VITA 48 [23]. The HVPS provides static and dynamic high voltage potentials to drive the ECP and WPS space environment sensors. The ECP sensor requires static high voltage to provide operational bias to the solid-state detectors. The WPS requires a stepping high voltage supply to sweep the EA filter plate from -10V to -5kV and static voltages to bias the MCP and transmissive grid.

The design supports a Space-Wire Interface on the control and expansion planes as well as an I2C interface on the system management bus enabling development with low-cost commercial enclosures, backplanes, and other resources that have been leveraged during the design process. The flight power supply will support two unipolar high voltage outputs up to 5 kV DC. The design leverages a common control interface to allow the substitution of different high voltage multiplier and/or transformer configurations to tailor the output voltage and current drive capability. The design meets the mission radiation hardness requirements for operation in GTO by employing radiation hardened components with >100 kRad (Si) tolerance. The digital interface and control will be implemented using a SAMRH707 microcontroller running the FreeRTOS Real Time Operating System (RTOS) and a Lattice Field Programmable Gate Array (FPGA). High voltage outputs will be connected using an appropriately rated front panel connector.

Control of the HVPS is performed digitally across the DPM's FPGA and microcontroller. The FPGA interfaces directly with the drive circuitry on the HV section of the power supply. A comparator detects the timing of resonant oscillation to optimize power delivery through pulse width modulation and a DAC control drive strength. The microcontroller can access control and status registers located on the FPGA via a Space-Wire connection between the two. The HVPS output voltage sense is read by a 12-bit SAR ADC within the FPGA at 177.5 kHz on each channel, followed by cascaded integrator-comb (CIC) filter and optional FIR filter. The CIC filter allows additional ADC resolution while the input is decimated to a control rate closer to the resonant frequency [23].

Bench-top testing of the prototype has been conducted to verify the ability of the control algorithm to command the stepping voltage using 100 V steps, see Figure 5. The slew rate of the controller with a 100 MΩ/530 pF test load is 19 V/ms. Controller step times are <50 ms for 100 V and <100 ms for 1k V steps. Steady-state ripple is +/- 2.5 V for setpoints between 1 and 2.5 kV.

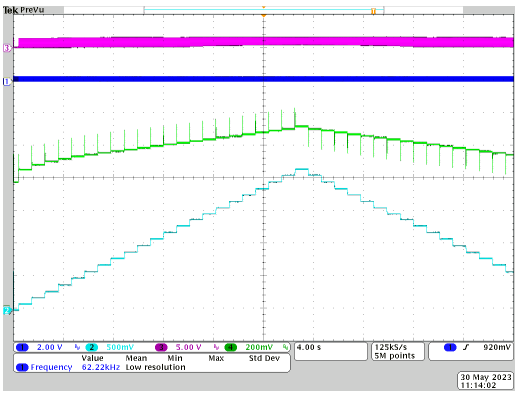

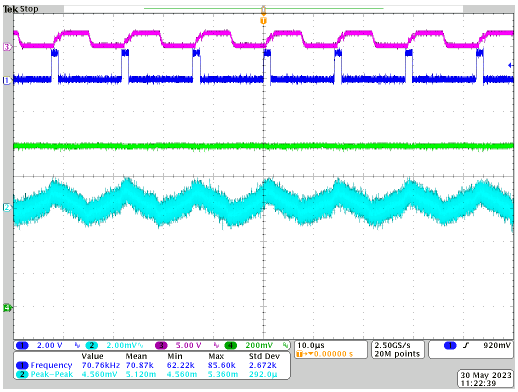

**Figure 5. Stepping voltage control with 100 V steps (top) and steady state performance at 1 kV (bottom). Light blue: HV output 1mV=1V, green: DAC bias, dark blue: PWM drive, magenta: comparator output.**

### *Distributed Processor Module (DPM)*

The ESRA mission serves as a risk-reduction flight for the distributed architecture concept [2]. Although ESRA is a 12U CubeSat with sensors and subsystems co-located, the WPS and ECP sensors are designed as "smart" sensors to obtain flight heritage for the distributed concept. The key enabling technology in ESRA is the distributed processor module (DPM). The DPM is essentially a re-usable reference design for low-power digital electronics at the sensor head.

Space system architectures traditionally utilize a backplane in an enclosure to provide a central hub for command, data handling, processing, and power distribution. Network-based architectures, such as Open/SpaceVPX, enable alternate solutions. The traditional enclosure can be split into physically separated sub-instruments that stand-alone mechanically and are tethered to a smaller less resource-intensive hub. This distributed architecture concept provides flexibility and adaptability when integrating to mechanical and electrical requirements of a particular host. A distributed system adds more modularity and the flexibility to add or subtract individual payloads from a primary payload hub without leaving empty backplane slots in the larger enclosure. Furthermore, this distributed processing concept enables "smart" sensors – self-contained sensors with data processing at the head, which are easier to test, integrate and re-use.

The two primary components of the DPM are the SAMRH707 microcontroller and the Lattice Certus-NX LFD2NX-40 radiation-tolerant FPGA. Note, the Vorago VA41630 radiation-hardened Arm Cortex-M4 microcontroller was replaced by the SAMRH707 due to compatibility and integration issues. The microcontroller features 256 KB of internal Ferroelectric Random Access Memory (FRAM), 320 KB of internal Static random-access memory (SRAM), integrated error-detection and correction (EDAC), a single-precision floating-point unit, a direct memory access controller, an external bus interface, a two port Space-Wire router, a 10/100 Ethernet media access controller, an 8-channel 600-kSPS 12-bit ADC, a 2-channel 12-bit DAC and a variety of serial interfaces. The FPGA features 40k equivalent logic cells, a 1.25 Gbps SerDes and an 18-channel 1-MSPS ADC. The reference design also includes an assortment of optional radiation-hardened/tolerant supporting memories, including a 64-Mbit parallel flash, 16-Mbit SRAM, and 64-Mbit serial flash. The ESRA payload utilizes the DPM within the WPS and ECP sensors as well as the HVPS and LVPM sub-systems.

### *Low Voltage Power Monitor (LVPM)*

The primary function of the LVPM is to handle power management of the ESRA CubeSat instrument subsystems. It monitors voltage and current provided to each subsystem and sends discrete signals to enable/disable power to each subsystem. This strategy allows for configurable power modes. A high-power mode that provides power to all subsystems, a low-power mode that powers the DPM to preserve volatile memory, and multiple customizable power modes as needed.

If load shedding becomes necessary, a custom power mode can be commanded. The Payload Processor (PP) issues these commands to the LVPM to change between predetermined power modes or change power states of individual subsystems. The PP can make these decisions utilizing power consumption and quality data reported by the LVPM. In the event of an instrument fault being detected, the LVPM will autonomously remove power to a subsystem to ensure power stability of the rest of the system. This is a critical capability to prevent catastrophic failure resulting from a possible single event latch-up (SEL) due to radiation effects. The LVPM will also contain a microdosimeter to measure total ionizing dose within the electronics box and monitor system health [24]. An engineering magnetometer is also included to inform background magnetic field models used in operations.

The LVPM design includes a switched mode power supply (SMPS) that draws power through direct battery access, and is meant to mitigate risk of mission data loss from volatile memory on the PP. In the event of a space vehicle power upset, the SMPS provides power only to the PP to preserve data captured by the mission for as long as possible. The battery voltage is monitored by an analog comparator and reference, which ensures that the

SMPS will be disabled before the critical battery voltage is reached.

### *Payload Processor*

The ESRA payload processor (PP) is a combination of 3U SpaceVPX and OpenVPX Architecture based on an existing LANL 6U design, enabling design reuse for firmware and flight software [25, 26, 27, 28]. The design employs a compact 3U Eurocard and Open/SpaceVPX architecture to reduce form factor while increasing performance. The reduction in size is critical for implementation on nano- and micro-satellite platforms such as the ESRA bus. The OpenVPX portion of the ESRA PP enables easier firmware and software development and testing by providing compatibility with cheaper commercial chassis, while the SpaceVPX portion allows for Space-Wire connectivity and critical signal redundancy.

The heart of the PP is the GR740 LEON4 SPARC V8 processor from Frontgrade/Gaisler. It is capable of gigaflop performance at the nominal 250 MHz clock rate. One Gbyte of synchronous dynamic random-access memory (SDRAM) with 512 Mbytes of EDAC, clocked at 25 MHz, is addressed by the processor for volatile program and data storage. Eight Mbytes of nonvolatile magnetoresistive random-access memory (MRAM) are also included for nonvolatile program memory storage.

Interface logic is primarily coordinated in the RTG4 FPGA from Microchip, running at a nominal 50 MHz. This includes discrete IO, UART, three Space-Wire endpoints, and a processor interface. Additional memory is addressable by the FPGA, including 256 Mbytes of DDR2 (not used on ESRA) and 1 Gbyte of NAND flash used for nonvolatile data storage. See Figure 6 for a block diagram of the Payload Processor.

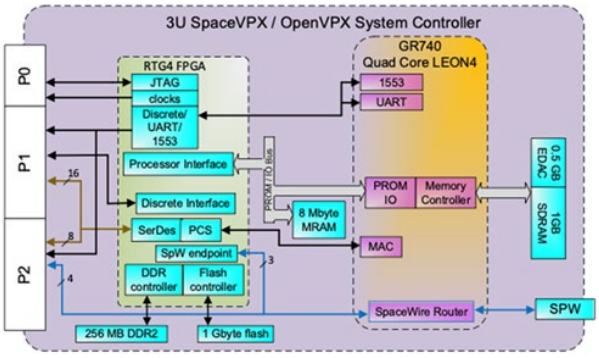


**Figure 6. Block diagram of the payload processor design [2].**

### *Flight Software (FSW) Architecture*

The ESRA FSW running on the Gaisler LEON4 payload processor is based on a modular publish-subscribe architecture. The foundation of the FSW is a message bus created by LANL's internally-funded Cubesat Reusable Interface Software Platform (CRISP) project [29] which provides an extremely lightweight architecture that supports messaging to and from all the different components of the software system. The message passing architecture has been extended to seamlessly communicate with the DPM over SpaceWire to the WPS and ECP smart sensors, and via I2C to the HVPS sub-system. The ESRA FSW on the Gaisler LEON4 payload processor has been designed to be modular and reusable, allowing future LANL missions to focus on mission-specific software components while simply reusing the existing capabilities from ESRA/CRISP. The ESRA payload processor FSW provides the command and data handling functionality for the entire payload and has been designed to tolerate upsets and reboots of the space vehicle. Science data, state of health, and log data are stored in both volatile SDRAM and mirrored to a non-volatile flash drive. Various payload configuration parameters are held in non-volatile MRAM along with a ground configurable time-tagged sequence of commands. By managing the commands and data in the payload's radiation tolerant memories, ESRA is better prepared for unexpected upsets to the space vehicle.

The space vehicle (SV) interface of the ESRA payload processor FSW has met the specifications of the NanoAvionics 12U CubeSat spacecraft bus. The SV interface communicates with the NanoAvionics bus using the CubeSat Space Protocol (CSP). This lightweight network layer delivery protocol is used to transmit and receive messages with the CRISP message bus. These messages can be commands coming from the ground or payload telemetry being sent to the ground. The ESRA payload processor FSW leverages an open-source CSP library developed at Aalborg University and nanosatellite provider GomSpace. This runs on top of the open source RTEMS operating system. The ESRA FSW running on the SAMRH707 in each instance of the DPM is built on top of the FreeRTOS real-time operating system.

The combined payload processor and DPM software system has been designed to handle both raw 'list mode' data and binned histogram data. For the WPS instrument, histogramming and voltage stepping has been implemented in the instrument's microcontroller software whereas for the ECP instrument histogramming has been implemented in the Lattice FPGA.

## MISSION DESIGN

A 12U commercial satellite bus provided by NanoAvionics will serve as the platform for the WPS and ECP sensors along with the critical subsystems such as the HVPS, DPM, and Payload Processor. The mission launch and integration are being provided by the DoD Space Test Program and Mission Manifest Office with an anticipated GTO insertion in July 2025. The desired orbital parameters include perigee of 200 km, apogee of 36,000 km, and inclination of 40° ±20°. The avionics and critical subsystems have flight heritage from the NanoAvionics M6P mission. NanoAvionics will assemble the 12U bus at its facilities and the final assembly, integration, and testing efforts will be carried out at LANL facilities. The 12U bus matches LANL's mission requirements and shares the same flight-proven subsystems as NanoAvionics' flagship M6P bus, but with up to 10U payload volume. The larger volume is needed to provide enough room for the ~10 kg LANL payload. The CAD model of the vehicle is shown in Figure 7 with critical systems indicated.

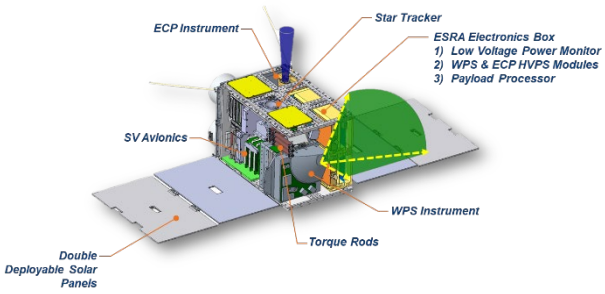


**Figure 7. Mechanical design illustrating the configuration of the ESRA bus.**

Note, the electronics box is mounted along the passive thermal radiator. This configuration was chosen because it optimizes thermal dissipation for the LANL payload processor, the largest heat source within the system. The orientation of the WPS and ECP sensors are optimized for their respective measurements. During nominal science operations, solar panels will face the Sun, WPS will face away from the Sun, and ECP will face approximately perpendicular to the Earth's magnetic field lines.

The ESRA mission will require 1 Gbyte of data downlinked each day to transmit telemetry which will include state-of-health (SOH) and science data. To ensure an adequate downlink budget an analysis using System Tool Kit (STK) was conducted to provide estimates of access times per day for the example KSAT$^{lite}$ ground stations. The KSAT$^{lite}$ ground stations were used for this exercise as they have been tailored to meet small satellite and constellation requirements [30]. To provide a reasonable downlink estimate this analysis assumed a 3.3 Mbps S-band radio and a maximum ground station range of 8,000 km. Three KSAT$^{lite}$ ground stations located in Mauritas, Greece, and California were then selected for the STK simulations. Note that, slew rates that exceeded 20 deg/sec were ignored. With these STK model parameters the total access time exceeds 40 minutes per day which is sufficient to downlink 1 Gbyte of data per day.

## SUMMARY

The ESRA mission will fly through GTO while making observations of the charged particle populations in the Earth's radiation belts. This will allow for the demonstration and validation of the next generation space environment sensors and critical subsystems. A commercial satellite bus supplied by NanoAvionics will host the WPS and ECP sensors along with the critical subsystems such as the HVPS, DPM, and Payload Processor. The mission launch and integration are being provided by the DoD Space Test Program and Mission Manifest Office with an anticipated GTO insertion in summer of 2025. The desired orbital parameters include perigee of 200 km, apogee of 36,000 km, and inclination of 40° ±20°. The commercial space sector continues to increase the capability of SmallSat platforms and ground stations while simultaneously reducing risk and cost. The ESRA mission leverages this capability by partnering with NanoAvionics, thus allowing the mission team to focus primarily on payload development.

### *Acknowledgments*

The research conducted at Los Alamos National Laboratory was under the auspices of the Department of Energy.

### *References*

[1] C. A. Maldonado et al., "The Experiment for Space Radiation Analysis: Probing the Earth's Radiation Belts Using a CubeSat Platform," in *Proceedings of the 36th Annual Small Satellite Conference*, Logan, UT, 2022.

[2] C. A. Maldonado, J. Deming, B. N. Mosley, K. S. Morgan, J. McGlown, A. Nelson, P. Fernandes, M. Kroupa, K. Katko, M. P. HHehlen, D. Arnold, J. Barney, C. Safi, M. Pyle, T. Schultz, D. Reisenfeld, R. Skoug, A. Guider, M. Holloway, H. Morning, E. Krause, B. Sandoval, D. Beckman, Z. Miller, R. Merl, P. S. Graham, T. P. White, Z. Tripp, B. Hoose, C. Roecker, A. Klimenko, R.

Dutch, K. Kaufeld, E. Cox, Q. Cole, C. Clanton, P. Bloser, B. A. Larsen, T. Fairbanks, J. George and J. Michel, "The Experiment for Space Radiation Analysis: A 12U CubeSat to Explore the Earth's Radiation Belts," in *IEEE Aerospace Conference*, Big Sky, MT, 2022.

[3] C. A. Maldonado et al., "Development of the Experiment for Space Radiation Analysis (ESRA) CubeSat Mission to GTO," in *IEEE Aerospace Conference*, Big Sky, MT, 2023.

[4] C. A. Maldonado et al., "The Experiment for Space Radiation Analysis (ESRA) - Technology Maturation of Next Generation Charged Particle Detectors in GTO," in *Advanced Maui Optical and Space Technologies (AMOS) Conference*, Maui, HI, 2022.

[5] D. Young, "Space plasma particle instrumentation and the new paradigm: Faster, cheaper, better," in *Measurement Techniques in Space Plasmas: Particles*, R. Pfaff, J. Borovsky and D. Young, Eds., Geophysical Monograp Series 102, 1998, pp. 1-16.

[6] C. Escoubet, R. Schmidt and M. Goldstein, "Cluster - Science and Mission Overview," in *The Cluster and Phoenix Missions*, Dordrecht, Springer, 1997, pp. 11-32.

[7] J. L. Burch, T. E. Moore, R. B. Torbert and B. L. Giles, "Magnetospheric Multiscale Overview and Science Objectives," *Space Science Reviews,* vol. 199, pp. 5-21, 2016.

[8] V. Angelopoulos, "The THEMIS mission," *Space Science Review,* vol. 141, pp. 5-34, 2008.

[9] J. C. McDowell, "The Low Earth Orbit Satellite Population and Impacts of the SpaceX Starlink Constellation," *The Astrohpysical Journal Letters,* vol. 892, no. 2, pp. 1-10, 2020.

[10] J. Radtke, C. Kebschull and E. Stoll, "Interactions of the space debris environment with mega constellations—Using the example of the OneWeb constellation," *Acta Astronautica,* vol. 131, pp. 55-68, 2017.

[11] D. Tournear, "Future Directions: Delivering Capabilities," in *Proceedings of the Small Satellite Conference, SSC20-IV-02*, Logan, UT, 2020.

[12] B. Braun, S. Sims, J. McLeroy and B. Brining, "Breaking (Space) Barriers for 50 Years: The Past, Present, and Future of the DoD Space," in *AIAA/USU Conference on Small Satellites*, Logan, UT, 2017.

[13] J. Barney, D. Arnold, O. Garduno, M. Kroupa, C. A. Maldonado, Z. Miller, C. Roecker, D. Wakeford and B. A. Larsen, "Experiment for Space Radiation Analysis, Energetic Charged Particle Sensor: a Charged Particle Telescope with Novel Sensors for Measuring Earth's Radiation Belts," in *IEEE Aerospace Conference*, Big Sky, MT, 2022.

[14] A. Gula, D. Arnold, J. Barney, K. Boyd, M. Caffrey, M. Holloway, M. Kroupa, B. A. Larsen, C. A. Maldonado, S. Mendel, Z. Miller and R. Simms, "Development of the Energetic Charged Particle Instrument for the ESRA CubeSat Mission," in *IEEE Aerospace Conference*, Big Sky, MT, 2023.

[15] Z. Miller, B. Stidham, T. Fairbanks and C. A. Maldonado, "The use of stereolithography (SLA) additive manufacturing in space-based instrumentation," in *IEEE Aerospace Conference*, Big Sky, MT, 2023.

[16] R. M. Skoug, H. O. Funsten, E. Mobius, R. W. Harper, K. H. Kihara and J. S. Bower, "A wide field of view plasma spectrometer," *J. Geophys. Res. Space Physics,* vol. 121, pp. 6590-6601, 2016.

[17] C. Carlson, D. Curtis, G. Paschmann and W. Michael, "An instrument for rapidly measuring plasma distribution functions with high resolution," *Adv. Space Res.,* vol. 2, no. 7, pp. 67-70, 1983.

[18] O. Siegmund, M. Gummin, J. Stock, D. Marsh, R. Raffanti and J. Hull, "High-resolution monolithic delay-line readout techniques for two dimensional microchannel plate detectors," San Diego, CA, United States, 1993.

[19] O. Siegmund, M. Gummin, J. Stock, G. Naletto, G. Gaines, R. Raffanti, J. S. Hull, R. Abiad, T. Rodriguez-Bell, T. Magoncelli, P. Jelinsky, W. Donakowski and K. Kromer, "Performance of the double delay line microchannel plate detectors for the Far-Ultraviolet Spectroscopic Explorer," in *Proc. SPIE 3114, EUV, X-Ray, and Gamma-Ray Instrumentation for Astronomy VIII*, San Diego, CA, 1997.

[20] O. Siegmund, M. Gummin, T. Sasseen, P. Jelinsky, G. Gaines, J. Hull, J. Stock, M. Edgar, B. Welsh, S. Jelinsky and J. Vallerga, "Microchannel plates for the UVCS and SUMER instruments on the SOHO satellite," in *Proc. SPIE 2518, EUV, X-Ray, and Gamma-Ray Instrumentation for Astronomy VI*, San Diego, CA, United States, 1995.

[21] O. Siegmund, P. Jelinsky, J. Stock, J. Hull, D. Doliber, J. Zaninovich, A. Tremsin and K. Kromer, "High resolution cross delay line detectors for the GALEX mission," in *Proc. SPIE 3765, EUV, X-Ray, and Gamma-Ray Instrumentation for Astronomy X*, Denver, CO, United States, 1999.

[22] O. Siegmund, B. Welsh, J. Vallerga, A. Tremsin and J. McPhate, "High-Performance microchannel plate imaging photon counters for spaceborne sensing," in *Proc SPIE 6220, Spaceborne Sensors III, 622004*, Orlando, FL, USA, 2006.

[23] J. Deming, E. Krause, A. Kirby, B. Sandoval, D. Beckman, Z. Miller and C. A. Maldonado, "A compact modular high voltage power supply for space applications," in *IEEE Aerospace Conference*, Big Sky, MT, 2023.

[24] C. Maldonado, R. Cress, P. Gresham, J. Armstrong, G. Wilson, D. Reisenfeld, B. Larsen, R. Balthazor, J. Harley and M. McHarg, "Space radiation dosimetry using the integrated Miniaturized Electrostatic Analyzer - Reflight (iMESA-R)," *Space Weather,* 2020.

[25] R. Merl and P. Graham, "Radiation-Hardened SpaceVPX System Controller," in *2018 IEEE Aerospace Conference*, Big Sky, MT, 2018.

[26] R. Merl and P. Graham, "MicroTCA for Space Applications," in *2016 IEEE Aerospace Conference*, Big Sky, MT, 2016.

[27] R. Merl, E. Cox, R. Dutch, P. Graham, S. Larsen, J. Michel, J. Milby, K. Morgan and K. Tripp, "LEON4 Based Radiation-Hardened SpaceVPX System Controller," in *2020 IEEE Aerospace Conference*, Big Sky, MT, 2020.

[28] R. Merl and P. Graham, "A low-cost, radiation-hardened single-board computer for command and data handling," in *2016 IEEE Aerospace Conference*, Big Sky, MT, 2016.

[29] R. Scobie, K. Kaufeld, B. Hoose, K. Morgan, K. Katko, M. Hehlen and J. Michel, "CubeSat Reusable Interface Software Platform (CRISP): A Lightweight Message-Bus-Based Flight Software Architecture for Rapid Payload Integration," in *Proceedings of the 36th Annual Small Satellite Conference*, Logan, UT, 2021.

[30] KSAT, "KSAT lite," KSAT Kongsberg Satelliet Services, [Online]. Available: https://www.ksat.no/ground-network-services/ksatlite/. [Accessed 7 June 2022].